

Pasture Monitoring Applying Normalized Difference Vegetation Index (NDVI) Time Series with Sentinel-2 and Landsat 8 Images, to Improve Milk Production at Santa Mónica Farm, Imbabura, Ecuador

Garrido Fernando(✉) and Caranqui Víctor

Department of Software Engineering and Artificial Intelligence,
Faculty of Engineering in Applied Sciences, Technical University of the North,
Avenue 17 de Julio 5-21, Ibarra, Ecuador
{jfgarridos,vcaranqui}@utn.edu.ec

Abstract. The soils have had an increasing pressure due to the intensification of their use for agriculture, forestry, grazing and urbanization. In this way, the implementation of good practices for sustainable soil management are essential to reverse their tendency to degradation as preventive measures and so, guarantee food security and protect the provision of different ecosystem services associated with the soil. The advent of the Sentinel and Landsat satellite programs provide free data sets with good spatial and temporal resolution that can be a valuable source of information for monitoring pasture resources. In order to evaluate this type of techniques, a time series (TS) was generated with images of the Landsat 8 (L8) OLI (*Operational Land Imager*) sensor and a time series with images of the Sentinel-2 (S2), MSI (*Multispectral Imager*) sensor to determine the best results in the quantification of changes in the coverage of pastures at the Santa Mónica farm. In this study, pastures were analyzed using the normalized difference vegetation index (NDVI) time series obtained from median quarterly mosaics obtained in 2019. Different samples were drawn that represent the change trend throughout the time series and were classified according to their degree of change and persistence in the series. The results indicate that the densification of the time series allows to provide better results in the quantification of the changes and dynamics of the coverage. The established methodology represents a great advance on the generation of images and the monitoring and detection of changes in coverage through time series [22]. Hence, it is one the first studies carried out in the country that incorporate this type of process. It was concluded that the determination of spectral signatures with the index used together with the near infrared (NIR) and short wave infrared (SWIR 1) spectral bands, allow to extract values and intervals where the change produced by pastures is identified with an acceptable level of accuracy.

Keywords: Sentinel-2 · Landsat 8 · Pastures · Vegetation index · Livestock · Teledetection · Remote sensing · Time series

© Springer Nature Switzerland AG 2020
O. Gervasi et al. (Eds.): ICCSA 2020, LNCS 12254, pp. 560–575, 2020.
https://doi.org/10.1007/978-3-030-58817-5_41

1 Introduction

Livestock in Ecuador depends on grazing, in this scope pastures are more than the cheapest food available for livestock feed. They offer all the necessary nutrients for good animal performance. Therefore, everything that can be done to improve the pasture production technology will directly result in milk production. Pasture management, together with local climatic conditions will affect pasture productivity and quality, and therefore agricultural production.

Therefore, there is a need for regular forage monitoring and prediction of pasture growth rates, providing milk producers who practice controlled or rotary pasture grazing systems, which consists of rotating livestock within the Soil, to avoid compacting soils (especially in the rainy season), in this way the soil is allowed to rest and improves the regrowth of grasslands. The way grazing in which is managed has a major impact on the physical [2], chemical and biological properties of soils. If lawn quantity and quality can be determined from space (i.e. via satellite), with adequate precision and spatial/ temporal resolution. This opens up a number of possibilities for more efficient pasture management and a more profitable pasture farming [4].

The number of satellite Earth observation systems is increasing and therefore the information available to users is increasing. Higher resolution, cloud-free, imagery, such as captured by Landsat 8 (L8) and Sentinel-2 (S2) [6], provides excellent information on surface heterogeneity and vegetation extent, but it cannot provide adequate multi-angle observations to accurately capture the true effects of surface anisotropy [7].

The use of remote sensing for monitoring and predicting forage crops used for grazing or silage in animal and dairy production systems is not well established due to the fact that intensive grazing pastures are highly dynamic systems and grass need to be carefully kept at the optimum height to avoid overuse of grassland. Despite these limitations, there have been notable investigations mainly in the use of the time series Normalized *Difference Vegetation Index* (NDVI) [8].

The objective of this research is to determine to what extent L8 and S2 are compatible in the construction of time series of vegetation indexes for identification and monitoring of pastures and to present the results of the verification of robust algorithms that can be applied to a variety of pasture types and throughout the growing season in three parcel categories (occupied, rest, and dry) that differ in pasture types and management regimen in Area Of Interest (AOI). For this reason, the Determination of Spectral Signatures in Crops is used, these spectral traces depend on the optical properties of the plants, which are also a function of various factors such as radiation conditions, plant species, the thickness of the leaves, the structure of the leaf surface, the levels of the chlorophyll content and the internal structure of the leaves.

As is well known, solar radiation is the primary source of energy for numerous biological processes that the crop has. Much of the solar radiation is absorbed by the plants or rather the leaves and is converted into heat and used to maintain its temperature and processes of thermal effects [18, 19]. The leaves have a first contact with radiation, the value of the light that is absorbed or transmitted between the leaves depends on their wavelength and the absorption selectivity of the leaf pigments [9]. The analysis of spectral signatures of pasture crops is carried out with the help of

geographic information system tools to obtain the characteristics of electromagnetic radiation with the structure of the pasture. The spectral signatures of pastures of the Regions of Interest (ROIs) or Training Areas are used.

2 Methods and Materials

2.1 Study Site

The present investigation was carried out at "Santa Mónica" farm, a property belonging to the Universidad Técnica del Norte, located 14 km from Ibarra city, in the area of Ilumán, in Imbabura province (0°17′N, 78°14′W). It has a perimeter of 106.7 hectares which is currently used for planting pastures and forage for around 300 dairy cows.

Its relief corresponds to an area mainly on slopes and extends in the central and southern part of the study area. The current use of the land is high with irrigation, exclusively for controlled or Intensive Rotary Beef Grazing. The frequency of permanence of the cattle in a single place depends on the existence and quality of the grass distributed in 96 hectares with 8 lots that oscillate between 0.5 and 3 hectares. The rest period is 20 days and the occupation period are 3 days. Additionally, 75% of the pastures at the farm are composed of Star grass (Cynodon nlemfuensis), the remaining 25% is found in Brachiarias species, such as decumbens and brizhanta (wire grass, bitter grass, hairy grass), in monoculture or mixed with Star. The predominance of pastoral use is found in the south west and south east of the study area, particularly in the lower parts and on slopes where important herds of cattle have been established. The study site is a combination with rest areas for grazing in the extreme south (named "reservorios" and "huertas"), where the cattle are grazed in pounding or folding (see Fig. 1).



Fig. 1. Santa Mónica farm: Location, Lots and Plots. Source: own illustration.

The climate of the study site corresponds to equatorial semi-humid mesothermal, with extreme variations between day and night, whose average annual temperature is approximately 15 °C, the minimum average being 9 °C and the maximum being

20 °C. It receives a greater amount of solar energy than a similar surface located at sea level due to its geographical location and height [32].

It allows global solar irradiation to reach high values throughout the year due to its location at zero latitude with an annual average of 533 cal/cm^2/day.

The average annual rainfall in this region is 852.8 mm, distributed in two rainy seasons (January to June and September to December), the dry months occur in July and August; relative humidity between 65 and 85%. However, there are also areas with low humidity. The average wind speed is 3 km/h. The driest month is July, with 16 mm of rain, and April is the warmest month of the year, and July is the coldest month of the year [33].

According to the study of the Agroecological Zoning of the study area between Pinsaquí and San Roque town, problems were identified, such as frost, hail, droughts, which hinder the development of crops, causing large losses, especially on the farm that requires grazing due to its dedication to milk production.

2.2 Controlled or Rotational Grazing

After a long period of pasture utilization, major changes in soil structure may occur such as compaction, which clogs the porous system, increases runoff and entrainment of particles, loss of organic matter, and decreased development of fine roots and, therefore, nutrient extraction [10].

Taking into account the economic and productive impact of degraded pastures on bovine production systems and the need to make decisions regarding the loss of pasture status and the absence of indicators that facilitate the implementation of the most relevant recovery practices, many milk producers use rotational grazing, where the interval or frequency of grazing (paddock rest) [1] is a function of the time the plant needs to regrow, recover organic reserves and complete the formation of green leaves. The density of the plant biomass makes it easier for cows to pluck the grass with their tongues to achieve large bite sizes and to facilitate the ingestion rate. On this subject Agnusdei [11], indicates that the consumption rates reach maximum values of 3.5–4 kg DM/h with heights greater than 18 cm; however, the consumption rates remained high (3 kg DM/h) in pastures of 15 cm and that the achievement of high intakes in dairy cows can be achieved both with high pastures (>15 cm) or with denser and lower pastures (<15 cm). The ideal meadow should have high availability and superior quality [12].

In order to establish a rotational grazing system, the systematic plan of rotations is established, that is, a regular sequence of periods of rest and periods of grazing or occupation of a series of grazing areas (set of plots or paddocks) is established in a cattle farm [13]. In this way it can be said that the number of paddocks and their formula to calculate it is given by Eq. (1):

$$\textit{Number of paddocks} = \frac{\begin{array}{c}\text{Rest period}\\ \text{appropriate for the grass}\end{array}}{\begin{array}{c}\text{Occupation period}\\ \text{of each group}\end{array}} + \text{number of grazing groups} \quad (1)$$

The rest period is given by the optimal time required by the plant species to restore, through photosynthetic activity, the carbohydrate levels required to ensure good regrowth. The occupation time, that is, the total time in which a pasture is grazed (by one or several groups of animals) must be short enough so that the animals do not eat the sprouts of the plants eaten at the end. grazing. Ideally, the animals should be removed from the lot, leaving such a proportion of young and active leaves that it is possible to continue using solar radiation and the adequate movement of reserving carbohydrates from the base of the plant and the root, in addition to protect the reproductive organs.

The grazing period is recommended not to exceed 8 days, since longer times of permanence of the animals in the pasture would affect the emergence of regrowth's, since there is the possibility that a plant is grazed more than once, with which it is it affects the individual production of the plant and the grassland and this is detrimental to its persistence [14]. The grazing period also depends on the number of animals and the type of animal that is used, for example, for a cow producing 18 L of milk it is appropriate to use 1-day grazing times, for cows of 10-12 L 2-3 grazing days would be indicated, while for cows of 6-8 L, grazing times may be used 4 day grazing [15].

The factors that influence the state of the pastures, obtained by the association of indicators of condition and water erosion, on the one hand with variables related to pasture management (establishment, height of pasture, age of pasture, days of occupation and rest, fertilization, herbal cleansing, pest management and animal load) and on the other, with biophysical variables (slope and altitude), were the slope, amount of seed sown at the time of establishment, days of occupation and rest. As a general rule, it is admitted that, from the height of the pasture at the time of pasture, 2/3 parts can be eaten by animals, while 1/3 part must be reserved for regrowth [12].

Many dairy farmers who practice rotational grazing systems generally track pasture productivity through the "field walk," to visually estimate grass biomass by simply estimating grass height. Therefore, this empirical way of measuring can lead to an inaccurate prediction of available lawn biomass with a consequent reduction in utilization efficiency [16].

2.3 Multispectral Satellites

There are several satellites with different characteristics that acquire multispectral images of the Earth's surface, they are particularly useful for monitoring land cover because the images are provided free of charge and can be downloaded directly from various platforms.

Landsat Satellites. Landsat is a set of satellites developed by NASA (*National Aeronautics and Space Administration of USA*) and the USGS (*United States Geological Survey*) [10], since the early 1970's, the launch of ERTS-1 (Earth Resources Technology Satellite, later renamed Landsat 1) began the era from a series of satellites that have since acquired continuous form of land data obtained by space-based remote sensing. The latest Landsat series satellite, the Landsat Data Continuity Mission (LDCM), was launched on February 11, 2013. Now renamed Landsat 8, the data

acquired by the satellite continues to expand the access for users from around the world [17].

The Operational Land Image (OLI) sensor and the Infrared Thermal Sensor (TIRS) presents the Landsat 8 satellite and the images consist of nine spectral bands with a 30-m spatial resolution of Bands 1 to 7 and 9. Ultra-blue band 1 is useful for cost and aerosol studies. Band 9 is useful for detecting cirrus clouds. The resolution of band 8 (panchromatic) is 15 m. Thermal Bands 10 and 11 are useful for providing the most accurate surface temperatures and are collected at 100 meters. The approximate size is 170 km scene from north to south by 183 km from east to west [6].

Sentinel-2 Satellite. The recent satellite program of the European Space Agency (ESA) [20, 21] of the Copernicus Sentinel-2 program comprises two satellites (2A, 2B) that ensure the continuity of the SPOT and LANDSAT programs and provide images with pixel size as fine as 10 m every five days (depending on latitude) [3]. The first Sentinel-2A satellite was launched on June 23rd, 2015, and the Sentinel-2B was launched on March 7th, 2017. The Sentinel-2B flies 180° opposite Sentinel-2A, with both spacecraft occupying synchronous orbits of the Sun at an altitude of approximately 786 km and covering Earth's land surfaces, large islands, inland and coastal waters of 84° N and 56° S [8]. It allows obtaining information on the two wavelengths, visible and infrared, allowing monitoring of changes in land and vegetation, as well as global monitoring of climate change [18]. It has an Multi Spectral Instrument (MSI) sensor that has 13 bands, of which four of them (in blue, green, red and near infrared) have 10 m of spatial resolution, six have 20 m of resolution that include bands on the red-edge and SWIR and the other three are 60 m for atmospheric correction and cloud detection.

The recent Sentinel-2 satellites in combination with Landsat (7 or 8), in both cases with freely available images [21], are ideal for monitoring pasture biomass availability on pasture farms and offer the opportunity to develop robust algorithms to exploit its potential in efficient and profitable pasture monitoring [5], and increase the possibilities of having time series data with higher spatial resolutions and denser, expanding the possibilities of its use in agriculture [19].

2.4 Classification of Land Cover

The objective of this study is to evaluate how different textural characteristics contribute to discriminate most types of vegetation and the state of pastures.

Vegetation Index. Vegetation analysis and detection of changes in vegetation patterns are key to the evaluation and monitoring of natural resources. So it is not surprising that the detection and quantitative evaluation of green vegetation is one of the main applications of remote sensing for natural resource management and decision making [22].

Chlorophyll is a pigment of plants, which gives them their green color and absorbs the light necessary for photosynthesis, energy strongly in the bands centered at 0.45 and 0.67 μm. That is why we perceive healthy green vegetation, due to the great absorption in blue and red by the leaves and the reflection in the green. When the vegetation is not healthy, the chlorophyll decreases, and the result is an increase in the

spectral reflectance in the red, making the leaves appear yellowish (a mixture of green and red). In vegetation, the level of reflectance is mainly modified by factors such as: the types of pigments, the structure of the leaves and the moisture content. The first affects wavelengths of the visible spectrum (0.4–0.7 m) where 65% is absorbed by Chlorophyll, 29% by Xanthophyll and 6% by Carotenes [23].

Additionally, changes in vegetation vigor and infrared imaging have been valuable in detecting and mapping the presence, distribution, and extent of diseased crops and insect infestations. In addition, changes in leaf structure that accompany the natural maturity of crops are subject to detection with infrared imaging [24]. The spectral signature characteristic of healthy vegetation shows a clear behavior between the red bands (0.6 to 0.7 μm) and the near infrared (0.7 to 1.1 μm). There is a notable spectral contrast between the RED band of the spectrum and that of the NIR, which allows separating healthy vegetation from other covers [26].

Normalized Difference Vegetation Index – NDVI. It is an index used to measure the normalized difference between Red and Near Infrared (near IR) reflectance's, providing a measure of the quantity, quality and development of vegetation cover and vigor in large areas [25]. The frequent use of the **NDVI** for studies like the one here has been carried out, is that the active vegetation has a different behavior in the Red and near IR bands: in the visible region of the electromagnetic spectrum, the pigments of the leaves absorb most of the energy they receive by minimally reflecting the received solar energy, while in the near IR the absorption is very low and therefore the reflectivity is much higher than in Red.

For this reason, a spectral contrast is produced between these bands, which allows the vegetation to be clearly separated from other coverings [27]. For the S2 image, three NDVIs were used as a result of the combination of the bands: 6-4, 7-4 and 8-4, since bands 6 and 7 are specifically located in the spectral region of the red margin, whose purpose it is to detect changes in the biological state of the pastures [28], while band 8 is already considered in the near IR. For L8 the NDVI was performed between bands 5-4 since in this sensor band 5 is in the near IR. It can be seen in Fig. 2 that the adjustment lines obtained between sensors for the NDVI indexes are slightly above the 1: 1 line. This means that in a same pixel the value of the NDVI index in Landsat would be above the value in Sentinel [19].

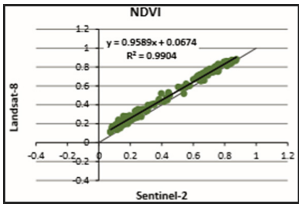


Fig. 2. NDVI relationship between Landsat-8 and Sentinel-2. Source: illustration based on [19].

The NDVI at L8 and S2 is calculated using the following expression [25]:

$$\begin{aligned} NDVI &= (B5 - B4)/(B5 + B4)\,\text{Landsat 8} \\ NDVI &= (B8A - B4)/(B8A + B4)\,\text{Sentinel - 2} \end{aligned} \tag{2}$$

The range of the NDVI value varies between −1 and 1. Due to the strong relationship between this index and the photosynthetic activity of plants, this index is widely used to analyze the condition of vegetation, biomass, vegetation cover, among others.

Landsat 8 and Sentinel-2 Bands Color Composition. A band composition is an image made up of the combination of three different bands of the sensor and each arranged in the three projection channels on the screen: Red (R), Green (G) and Blue (B). The RGB scene results in a color image and they are: infrared, false color for urban detection, atmospheric penetration analysis, natural color, vegetation analysis, Normalized Differential Water Index (NDWI), Normalized Difference Snow Index (NDSI), Enhanced Vegetation Index (EVI).

Automatic Classification. The classification process, in the context of remote sensing, consists of assigning to each pixel of the original image a label corresponding to one of the classes that we either predefine prior to the classification process or, due to the similarity of the characteristics of the pixels of the image to classify, are automatically grouped in the process. For this, classifiers are used, defined as methods, criteria or algorithms that are used as a mechanism to assign these pixels or segments to each category [31].

Classes and Macro Classes. Land cover classes are identified with an arbitrary ID code (identifier). SCP (Semi-Automatic Classification Plugin) [30] allows creating ROIs defining the Classes and Macro classes. Each ROI is identified with a class ID (C) and each ROI is assigned to a land cover class through a macro class ID (MC). Macro classes are integrated of various materials that have different spectral signatures; to achieve good classification results, the spectral signatures of different materials must be separated, even if they belong to the same macro class. Therefore, multiple ROIs will be created for each macro class (setting the same MC macro class ID but assigning a different class ID (C) for each ROI). Table 1 shows the macro classes and classes created for this study.

Table 1. Macro Classes and classes of the AOI Santa Mónica farm.

Name Macro class	Macro class ID	Name class	Class ID
Pastures	1	Resting pastures	1
Pastures	1	Active pastures	2
Vegetation	2	Gully	4
Vegetation	2	Undergrowth	5
Pastures	1	Dry pasture	3
Source: own elaboration			

Therefore, Classes are subsets of a Macro class, as shown in Fig. 3.

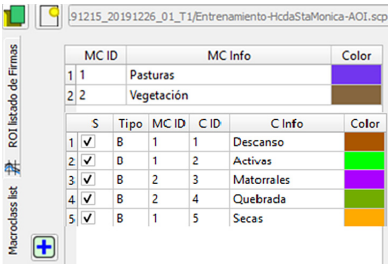


Fig. 3. List of signatures of the training areas at Santa Mónica farm; source: own study.

Spectral Signatures. Once electromagnetic energy reaches the earth's surface, it interacts with each type of material, either by reflection, absorption, or transmission, according to a spectral response pattern. This distinctive behavior of each type of material is exploited in image classification processes, and it is common to refer it as "spectral signature" [31].

If the spectral behavior of the plant canopy is analyzed, healthy vegetation offers low reflectivity in the red band of the spectrum (between 600 and 700 nm) and high in the near infrared (between 800 and 1000 nm), so that the higher the "vigor" the vegetation presents, the greater the contrast between the reflectance values captured in both bands [23].

Spectral Distance. It is useful to assess the spectral distance (or separability) between training signatures or pixels to assess whether different classes that are very similar to each other could cause classification errors. The Euclidean Distance has been used in this study, which is particularly useful for evaluating the results of the minimum distance classification. The Euclidean Distance is calculated from the center of the source cell to the center of each of the surrounding cells. Conceptually, the Euclidean algorithm works as follows: for each cell, the distance to each source cell is determined by calculating the hypotenuse with x_max and y_max as the other two sides of the triangle. This calculation derives the true Euclidean distance, rather than the cell distance. The shortest distance to an origin is determined, and if it is less than the specified maximum distance, the value is assigned to the location of the cell in the output raster (see Fig. 4).

	MC_ID = 1 MC_info = Pasturas C_ID = 1 C_info = Secas
	MC_ID = 1 MC_info = Pasturas C_ID = 2 C_info = Descanso
Jeffries-Matusita distance	n/a
Spectral angle	8.5377364625159 39e-07
Euclidean distance	3.644139862357838e-11
Bray-Curtis similarity [%]	99.99999973128634

Fig. 4. Spectral Distance between Dry Pastures and Rest Pastures of the AOI Santa Mónica farm. Source: own study.

2.5 Field Data Collection

The data of the study area were obtained during 2019 from the Sentinel-2 satellite [bands 2, 3, 4, 5, 6, 7, 8, 8A, 11.12] and from the Landsat 8 satellite [bands 2.3, 4,5,6,7], for this, Landviewer and Crop Monitoring satellite image platforms for remote sensing, applications developed by EOS DATA ANALYTICS, INC. [29]. With the images of the specified AOI (Area of Interest) it was possible to filter images by different criteria, mainly by year, month, percentage of cloudiness and solar elevation. Images with the highest spatial resolution ($\sim$0.5–1.5 m/pxl) as a separate data source. They also have a period of frequent data review ($\leq$ 1 day), which allowed controlling the conditions of the requested land surface.

The preliminary phase (cabinet) initially consisted of processing satellite images to identify: use, coverage, physiography of the terrain and access roads based on the following procedures.

Radiometric Correction. This procedure was performed to compensate for radiometric errors that may exist in the images. These errors are usually the result of defects in the operation of the sensors. Through radiometric correction, the image improved in its visual quality.

Resampling at 15 m. Landsat 8 images have the advantage of a panchromatic band with a spatial resolution of 15 m. This procedure allowed data from the multispectral reflection bands (1 to 5 and 7) with spatial resolution of 30 m to be resampled to 15 m.

Atmospheric Correction. Dark Object Subtraction (DOS), which is a family of image-based on atmospheric corrections [34], has been used for this study. Chavez [35] explains that "the basic assumption is that in the image some pixels are completely in shadow and, their radiation received from the satellite is due to atmospheric dispersion (haze effect). This assumption is combined with the fact that very few elements on the Earth's surface have an absolute black color. Therefore, an assumed reflectance of one percent is better than zero percent". The haze effect is given by Eq. (3) [36].

$$L_p = L_{min} - L_{DO1\%} \tag{3}$$

where:

L_{min} = ""radiance that corresponds to a digital value for which the sum of all pixels with digital values less than or equal to this value is equal to 0.01% of all pixels in the image under consideration" [37]. Therefore, the radiance obtained with that digital count value (DN_{min}).
$L_{DO1\%}$ = radiance of the dark object, with an assumed value of reflectance of 0.01.

In particular for Landsat images:

$$L_{min} = ML * DN_{min} + AL \tag{4}$$

Sentinel-2 images are converted to radiance before DOS1 calculation [30]. The Radiance of the Dark Object is given by Eq. (5):

$$L_{DO1\%} = 0,01 * [(ESUN_{\lambda} * \cos\theta_s * T_z) - E_{down}] * T_v/(\pi * d_2) \quad (5)$$

Therefore, the haze effect is:

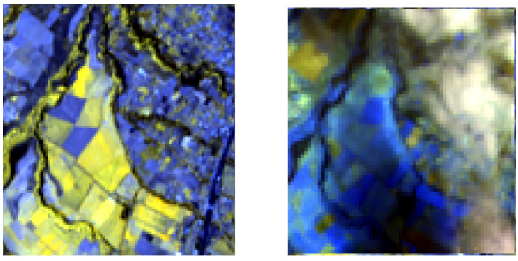
$$L_p = ML * DN_{min} + AL - 0,01 * [(ESUN_{\lambda} * \cos\theta_s * T_z) - E_{down}] * T_v/(\pi * d_2) \quad (6)$$

For Landsat 8, ESUN [38] can be calculated with Eq. (7):

$$ESUN = (\pi * d_2) * (\text{RADIANCE}_{\text{MAXIMUM}}/\text{REFLECTANCE}_{\text{MAXIMUM}}) \quad (7)$$

where RADIANCE_MAXIMUM and REFLECTANCE_MAXIMUM is provided in the image metadata.

Figure 5 It shows the atmospheric correction made to images S2 and L8 of our study area, using the DOS1 algorithm.



a) b)

Fig. 5. a) Atmospheric Correction DOS1 in S2 b) Atmospheric Correction DOS1 in L8 of the AOI Santa Mónica farm. Source: study illustration.

Time Series Analysis. The time series graph for the study in 2019 was performed to show data based on the values of the NDVI spectral index of satellite images with a minimum percentage of cloud cover. This graph (see Fig. 6), which is determined by the types of surface registered in the field of view of the satellite sensor, and the peak values depend on the meteorological parameters (temperature, humidity, cloudiness, etc.). So, it allowed to have a better knowledge of the health of the pastures and to identify at an early stage the stressed or infected vegetation.



Fig. 6. Time series graph based on NDVI of the AOI in 2019. Source: own study.

Digital Classification of the Image. The image improved with the indices found was digitally classified, this process was started with the recognition of spatial patterns, later the training or supervised classification was performed to recognize the patterns detected in the rest of the image, the purpose was mainly to detect areas with occupied pastures and waste pastures (rest or dry) (see Fig. 7).

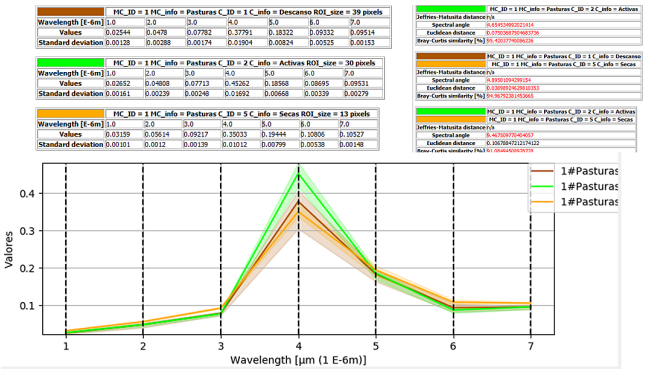


Fig. 7. Detail, distance, and spectral signature graph of the AOI Santa Mónica farm. Source: own study.

3 Results and Discussion

As observed in Fig. 7 which in the visible spectrum region has a low reflectance given the strong absorption by the foliar pigments. It is also observed that there is a change at the end of the wavelength of the red zone This characteristic is a spectral response of all vegetation, this is presented by the low reflectance of chlorophyll and the high reflectance in the near infrared, associated with the internal structure of each pasture and the water content. If the pastures in the study area were diseased, the carotenes and xanthophylls would be more dominant in the pastures, which could turn the pastures into a greater yellow influence since they absorb blue light and reflect green and red light. It does not happen in our spectral signatures. They are healthy pastures, they have a behaviour or pattern similar to the general spectral signature for vegetation. So, for instance in the near infrared zone the reflectance itself will reach remarkable values because the green leaves absorb the little energy of this region. However, in the mid infrared zone the spectral response will be dominated by the water of the plants and the high moisture content of green grasses, which give high absorption values and, therefore they lead to lower reflectance values, with this it is demonstrated how important is the determination of spectral signatures of crops.

In both satellites L8 and S2, the annual data of the NDVI was considered, the results shown in the dispersion graph (see Fig. 8) that the correlation analysis between the NDVI in active or occupied pastures indicates pastures healthy whereas for resting and dry pastures the correlation is weak because there is a high reflectance in the near infrared zone, which is basically associated with the internal structure of the pasture

and the water content, which have a significant association in each ecosystem, and they are influenced by the degree of seasonality of rainfall. An important factor in dry pastures that predominates is the roughness since the reflectance tends to increase along the wavelength and they have larger thresholds, which means that this transfer zone has a high standard deviation. It is in large thresholds there will be a heterogeneity of pixels that make up the firm, where it verifies that the grasses are dry and are not absorbing water. So, there is no longer any absorption of energy, it has this behavior of increasing reflectance at along the wavelength.

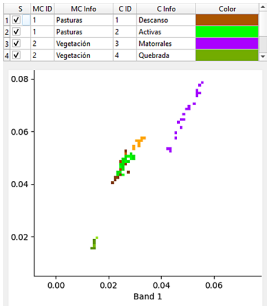


Fig. 8. Dispersion graph of the spectral signature of the AOI Santa Mónica farm. Source: own study.

Therefore, it is recommended to also identify new pasture species that have a sensitive growth to changes in solar radiation to more accurately infer NDVI.

4 Conclusions

A significant improvement has been achieved with respect to the time of occupation and the time of rest, the map obtained from pastures at Santa Mónica farm, applying digital and visual techniques of interpretation of Landsat 8 and Sentinel-2 images, is quantitatively reliable in 90% accuracy when the location and distribution of the mentioned coverage is shown.

The condition of the pastures evaluated in the areas of the farm showed that 73.3% are in good conditions (occupied pastures), the remaining 26.7% was divided into conditions: 20.5% regular (rest pastures), 3.6% bad (dry pastures) and 2.6% very bad (thickets) to direct the pasture to an optimal condition according to the characteristics in the place and production expectations, indicators that explain the condition of the pasture in agreement with the slope, coverage, vigor, and the presence of laminar erosion.

In our country, the main tool to increase milk production per hectare is precisely the animal load with well-managed pastures in the valleys of the mountains. It can sustain 4 UB/ha. On the other hand, the milk production potential of temperate pastures (without supplementation) is about 15–18 L in contrast to 8–10 L in tropical pastures.

The proposal of this document groups and incorporates innovations to the best practices and spectral artifacts of the most evaluated methodologies, generating a considerable level of milk productivity. We can say that the Sentinel-2 data, combined with a semi-automatic classification model, can be used to monitor pastures at high space-time resolutions and with reliable precision.

References

1. Altieri, M., Nicholls, C.: Agroecología Teoría y práctica para una agricultura sostenible. Programa de las Naciones Unidas para el Medio Ambiente, México D.F (México). Primera edición (2000)
2. Abecia, J.: La "ganadería de precisión" en el sector de los pequeños rumiantes. Ganadería, Nº. 95, pp. 34–37 (2015). ISSN 1695-1123
3. Drusch, M., et al.: Sentinel-2: ESA's optical high-resolution mission for GMES operational services. Remote Sens. Environ. **120**, 25–36 (2012)
4. Granados, F.: Uso de Vehículos Aéreos no tripúlados (UAV) para la evaluación de la producción agraría. Instituto de Agricultura Sostenible-IAS/CSIC (2011)
5. Punalekar, S.M., Verhoef, A., Quaife, T.L., Bermingham, L., Reynolds, C.K.: Application of Sentinel-2A data for pasture biomass monitoring using a physically based radiative transfer model. Remote Sens. Environ. **218**, 207–220 (2018)
6. Mishra, N., Md, O.H., Leigh, L., Aaron, D., Helder, D., Markham, B.: Radiometric cross calibration of Landsat 8 operational land imager (OLI) and Landsat 7 enhanced thematic mapper plus (ETM+). Remote Sens. **6**, 12619–12638 (2014)
7. Aguilar, H., Mora, R., Vargas, Ch.: Centro Nacional de Alta Tecnología, Costa Rica: Metodología para la corrección atmosférica de imágenes aster, rapideye, spot 2 y landsat 8 con el módulo flaash del software ENVI. Revista Geográfica de América Central. **53**, 39–59 (2014)
8. Bravo, N.: Teledetección espacial Landsat, Sentinel2, Aster l1t y Modis. 1ra. edición. Geomática Ambiental S.R.L., Huánuco, Perú (2017)
9. Benavides, M.F., Nieuwenhuyse, A., Villanueva, C., Ibrahim, M., Tobar, D., Robalino, J.: Capitulo 2 Evaluación de la condición de pasturas de Brachiaria Brizantha y su impacto económico en la producción ganadera en la cuenca media del río Jesús María, Costa Rica. Tesis Maestría de socio economía ambiental- CATIE (2017)
10. Avogadro, D., Padró, J.: Diferenciación de plantaciones forestales en entre ríos (Argentina): comparación de métodos de clasificación aplicados a imágenes Sentinel-2 y Landsat-8. Revista Internacional de Ciencia y Tecnología de la Información Geográfica. Departamento de Geografía, Universitat Autònoma de Barcelona Campus de Bellaterra, Cataluña, España (2019). http://dx.doi.org/10.21138/GF.652
11. Agnusdei, M.: Ecofisiología aplicada a pasturas. Unidad 1, Crecimiento de forraje. Grupo Producción y Utilización de Pasturas. Argentina: UI EEA INTA Balcarce, FCA UNM (2009)
12. León, R., Bonifaz, N., Gutiérrez, F.: Pastos y forrajes del Ecuador. Siembra y producción de pasturas. Editorial Universitaria Abya-Yala. Universidad Politécnica Salesiana. Quito - Ecuador (2018)
13. Godoy, P.: Desarrollo de un modelo espacial de riesgo de infección de fasciola hepatica en vacunos lecheros de la sierra central. Tesis para optar el grado de maestro magister Scientiae en Producción Animal, Lima, Perú (2018)

14. FAO. AGP - Praderas, pastizales y cultivos forrajeros. https://goo.gl/CsVaKw. Accessed 13 Aug 2019
15. Rincón, J.J.: Cuantas unidades animales por hectárea podemos manejar -PARTE 1 Conceptos básicos necesarios (2017) https://www.engormix.com/ganaderia-leche/articulos/cuantas-unidades-animales-hectarea-t41122.htm. 14 June 2019
16. Gebremedhin, A., Badenhorst, P., Wang, J., Spangenberg, G., Smith, K.: Prospects for Measurement of Dry Matter Yield in Forage Breeding Programs Using Sensor Technologies. Agronomy MDPI. (2019). https://doi.org/10.3390/agronomy9020065
17. ESA. Sentinel. S2 MPC Sen2Cor Software Release Note. Reference: S2-PDGS-MPC-L2A-SRN-V2.8.0 Issue: 02 (2019)
18. Díaz, J.: Estudio de Índices de vegetación a partir de imágenes aéreas tomadas desde UAS/RPAS y aplicaciones de estos a la agricultura de precisión. Trabajo fin de máster curso 2014–2015. Universidad Complutense de Madrid, Madrid, España (2015)
19. Tello, J., Gómez-Báguena, R., Casterad, M.A.: Comparación y ajuste en zonas agrícolas de índices de vegetación derivados de Landsat-8 y Sentinel-2. In: Ruiz, L.A., Estornell, J., Erena, M. (eds.) Nuevas plataformas y sensores de teledetección. XVII Congreso de la Asociación Española de Teledetección, pp. 81–84, Murcia, España (2017)
20. ESA (European Space Agency). http://www.esa.int/. Accessed 16 Feb 2020
21. USGS (U.S. Geological Survey). https://www.usgs.gov/. Accessed 10 Mar 2020
22. Zaraza, M.A., Manrique, L.M.: Generación de datos de cambio de coberturas vegetales en la sabana de Bogotá mediante el uso de series temporales con imágenes Landsat e imágenes sintéticas MODIS-Landsat entre los años 2007 y 2013. Revista de Teledetección Asociación Española de Teledetección (2019). https://doi.org/10.4995/raet.2019.12280
23. Hernández, H.: Procesamiento digital de imágenes. Universidad de Chile. (2011). ISBN 978-956-353-324-8
24. Chuvieco, E.: Teledetección Ambiental: La observación de la Tierra desde el Espacio, 3ra edición. Ariel Ciencia, Barcelona, España (2008)
25. Rouse, J., Haas, R., Schell, J., Deering, D.: Monitoring the vernal advancement and retrogradation (green wave effect) of natural vegetation. In: Fraden, S.C. (ed.) Third ERTS-1 Symposium, 10–14 December 1973, NASA SP-351, pp. 309-317. Goddard Space Flight Center Texas A&M University College Station, Texas (1974)
26. Maskova, Z., Zemek, F., Kvet, J.: Normalized difference vegetation index (NDVI) management of mountain meadows. Boreal Environ. Res. **13**, 417–432 (2008)
27. Soria, J., Granados, R.: Relación entre los índices de vegetación obtenidos de los sensores AVHRR del satélite NOAA y TM del Landsat. Ciencia Ergo Sum **12**(2), 167–174 (2005). Universidad Autónoma del Estado de México, México
28. Ju, C.H., Tian, Y.C., Yao, X., Cao, W.X., Zhu, Y., Hannaway, D.: Estimating leaf chlorophyll content using red edge parameters. Pedosphere **20**(5), 633–644 (2010)
29. LANDVIEWER. https://eos.com/lv/es/, https://eos.com/landviewer/?id=LE07_L1GT_010060_20200328_20200330_01_RT&b=Red,Green,Blue&anti&pansharpening&lat=-0.00195&lng=-77.26364&z=8. Accessed 03 Apr 2020
30. Congedo, L.: (SCP) Semi-Automatic Classification Plugin. Documentation. Versión 6.4.0.2 (2020). https://plugins.qgis.org/plugins/SemiAutomaticClassificationPlugin/
31. Carmelo, A., Moreno, A., Rodríguez, E.: Determinación experimental de la firma espectral de la vegetación. una sencilla práctica de introducción a la Teledetección. In: Avances y Aplicaciones. VIII Congreso Nacional de Teledetección, Albacete, España, pp. 429–432 (1999)
32. AccuWeather. https://www.accuweather.com/es/ec/national/satellite-wv. Accessed 24 Feb 2020
33. INAMHI. https://www.serviciometeorologico.gob.ec

34. Brizuela, A., Aguirre, C., Velasco, I.: Aplicación de métodos de corrección atmosférica de datos Landsat 5 para análisis multitemporal. Teledetección, Ed. Martin, UBA, Buenos Aires, Argentina (2007)
35. Chavez, J.: An improved dark-object subtraction technique for atmospheric scattering correction of multispectral data. Remote Sens. Environ. **24**, 459–479 (1988)
36. Tagestad, J.: Radiometric standardization of adjacent Landsat Thematic Mapper Image for multi-scene mosaics. Master of Science, Utah State University, Logan, Utah (2000)
37. Sobrino, J.A., Raissouni, N.: Toward remote sensing methods for land cover dynamic monitoring: application to Morocco. Int. J. Remote Sens. **21**, 353366 (2000)
38. GRASS GIS. https://grass.osgeo.org/, https://grass.osgeo.org/grass78/manuals/i.landsat.toar.html. Accessed 17 Sept 2019